

Exact epidemic dynamics for generally clustered, complex networks

Thomas House

May 1, 2019

Abstract

The last few years have seen remarkably fast progress in the understanding of statistics and epidemic dynamics of various clustered networks. This paper considers a class of networks based around a new concept (the *locale*) that allow exact results to be derived for epidemic dynamics. While there is no restriction on the motifs that can be found in such graphs, each node must be uniquely assigned to a generally clustered subgraph in this construction.

1 Introduction

Recent progress on exact analytic approaches to epidemics on clustered networks has been extremely fast. Models have been proposed based on households [17, 3, 4], and the more general concept of local-global networks [1, 2]. Another recent innovation has come from generalisations of random graph theory [13, 10, 8], and at the same time, general methods have been proposed for manipulation of master equations [16, 15]. These complement the traditional epidemiological approach to clustering based on moment closure [9] that has recently been applied graphs with more general motif structure [7].

This paper draws on much of this recent activity, making three main contributions. Firstly, a set of networks is defined using the new concept of a locale (which is distinct from the recently introduced concept of a role [8]) that have no restriction on the motifs that can be present. Secondly, exact epidemic dynamics are derived for these networks—the first time that manifestly exact results for transient epidemic dynamics of an infinite clustered network with non-homogeneous mixing outside the clusters have been derived. Finally, techniques are presented for practical efficient calculation of quantities of interest.

2 General Theory

2.1 Network generation

We start with the definition of a network (or graph—we use the terms interchangeably) G of size N as a set of nodes (vertices) $V \cong \mathbb{Z}_N$, which are indexed by $i, j, \dots \in \mathbb{Z}_N$, and a set of links (edges) $E \subseteq V \times V$. The information contained in a network can be encoded in an adjacency matrix $\mathbf{A} = (A_{ij})$, whose elements are given by

$$A_{ij} = \begin{cases} 1 & \text{if } (i, j) \in E, \\ 0 & \text{otherwise.} \end{cases} \quad (1)$$

Here we consider symmetric, non-weighted networks without self-links and so $A_{ii} = 0$, $A_{ij} = A_{ji}$.

We now present a model for network creation that is both more general than previous work, and also allows significant analytic progress to be made. This starts by defining a set of objects we call *stubby subnets*, which are indexed by type σ . A stubby subnet of type σ and size n_σ consists of three elements:

1. A set of nodes $v^\sigma \cong \mathbb{Z}_{n_\sigma}$;
2. A set of within-subnet links, $e^\sigma \subseteq v^\sigma \times v^\sigma$, with a within-subnet adjacency matrix \mathbf{a}^σ defined as for \mathbf{A} above;
3. A vector of ‘stubs’ \mathbf{s}^σ , such that $\forall i \in v^\sigma, s_i^\sigma \in \mathbb{Z}$.

A full network is then constructed in the following way. Firstly, we take a number $M_\sigma \gg 1$ of each stubby subnet type, such that the network size and nodes are given respectively by

$$N = \sum_{\sigma} M_{\sigma} n_{\sigma}, \quad V = \bigoplus_{\sigma} \bigoplus_{m=1}^{M_{\sigma}} v^{\sigma}. \quad (2)$$

Here we use tensor sums \oplus to represent the aggregation of subnet nodes without the removal of ‘duplicates’ that would be implicit in set-theoretic union. We can also apply this concept to the within-subnet links, providing one part of the full link set,

$$E_1 = \bigoplus_{\sigma} \bigoplus_{m=1}^{M_{\sigma}} e^{\sigma}. \quad (3)$$

The remainder of links are then provided by constructing a full vector of ‘stubs’ and connecting these using the standard Configuration Model [11].

$$\mathbf{S} = \bigoplus_{\sigma} \bigoplus_{m=1}^{M_{\sigma}} \mathbf{s}^{\sigma}, \quad E_2 = \text{ConfigurationModel}(V, \mathbf{S}), \quad E = E_1 \cup E_2. \quad (4)$$

In the limit where the network is sufficiently large, no duplicate links will be produced through the union of E_1 and E_2 , however for explicit generation of finite-size networks, the removal of duplicates implicit in (4) is commonly used.

Having defined such a network, it is straightforward to calculate degree distributions and clustering coefficients, since a node i from a stubby subnet of type σ has degree and clustering coefficient

$$d_i = s_i^\sigma + \sum_j a_{ij}^\sigma, \text{ and } \phi_i = \frac{(\mathbf{a}^\sigma)_{ii}^3}{d_i(d_i - 1)}. \quad (5)$$

From consideration of the standard configuration model, a giant component emerges within a network of this kind provided

$$\sum_\sigma M_\sigma D^\sigma (D^\sigma - 2) > 0, \text{ where } D^\sigma := \sum_{i=1}^{n_\sigma} s_i^\sigma. \quad (6)$$

Note that we have implicitly assumed that all stubby subnets are internally connected.

2.2 Invasion and final size

We now introduce a framework for the determination of whether a network of the kind considered can support the invasion of a species obeying *SIR* dynamics. To do this, we define the concept of a *locale*, which is a stubby subnet of type σ , together with an ‘origin’ node $o \in v^\sigma$. Clearly, there are at least $\sum_\sigma n_\sigma$ such locales to consider, although symmetries may reduce the effective number of these. Locale types are denoted using indices like $\lambda = (\sigma, o)$.

Invasibility of a network of the type under consideration (i.e. one constructed from stubby subnets) can therefore be considered by constructing a branching process on locales. If we define a ‘locale next generation’ matrix as the number of secondary locales infected by an initially infected locale early in the epidemic, then we can use the dominant eigenvalue of such a matrix to define a threshold parameter.

In order to do this, we need to define two dynamical quantities. The first of these is T , the probability that infection eventually passes across a network link where one node starts infectious and the other susceptible. The second is $P_\sigma(j|o)$, which is the probability that within the locale (σ, o) , where infection is first introduced to node o , that infection eventually reaches node $j \in v^\sigma$. The calculation of these two quantities depends on the precise dynamical system underneath the transmission process, but once they have been determined, the locale next generation matrix (interpreted as the expected number of locales of type $\bar{\lambda} = (\bar{\sigma}, \bar{o})$ created by a locale of type $\lambda = (\sigma, o)$ early in the epidemic) is given by

$$\mathcal{K}_{\bar{\lambda}\lambda}^L = T \frac{M_{\bar{\sigma}} s_{\bar{o}}^{\bar{\sigma}}}{s_{\text{tot}}} \left((s_o - 1) + \sum_{j \in v_\sigma \ominus o} P_\sigma(j|o) s_j \right), \quad (7)$$

where the total number of stubs in the network is

$$s_{\text{tot}} = \sum_\sigma M_\sigma \sum_{i \in v_\sigma} s_i^\sigma. \quad (8)$$

The locale basic reproduction number, which is different from the standard basic reproductive number R_0 , is then the dominant eigenvalue of this matrix

$$R_L := ||\mathcal{K}^L|| \quad . \quad (9)$$

By using a ‘susceptibility sets’ argument as in [3, 4], the final size of an epidemic can also be calculated using the following set of transcendental equations:

$$\begin{aligned} R_\infty &= 1 - \frac{\sum_\sigma M_\sigma \sum_{i \in v_\sigma} x_i^\sigma}{\sum_\sigma M_\sigma n_\sigma} \quad , \\ x_i^\sigma &= \pi_i^\sigma \prod_{j \in v_\sigma \ominus i} ((1 - P(i|j)) + P(i|j)\pi_j^\sigma) \quad , \\ \pi_i^\sigma &= \left((1 - T) + T \sum_{\lambda'} \frac{M_{\sigma'} s_{o'}^{\sigma'}}{s_{\text{tot}}} \tilde{x}_{o'}^{\sigma'} \right)^{s_i^\sigma} \quad , \\ \tilde{x}_i^\sigma &= \tilde{\pi}_i^\sigma \prod_{j \in v_\sigma \ominus i} ((1 - P(i|j)) + P(i|j)\pi_j^\sigma) \quad , \\ \tilde{\pi}_i^\sigma &= \left((1 - T) + T \sum_{\lambda'} \frac{M_{\sigma'} s_{o'}^{\sigma'}}{s_{\text{tot}}} \tilde{x}_{o'}^{\sigma'} \right)^{s_i^\sigma - 1} \quad . \end{aligned} \quad (10)$$

Here R_∞ is the proportion of the population that is ultimately infected by the epidemic, x_i^σ is the probability that the i -th node in a stubby subnet σ avoids infection during the epidemic and π_i^σ is the corresponding probability for avoidance of global infection. Variables marked with a tilde represent secondary locales in the susceptibility-set branching process, and other quantities are as defined above.

2.3 Full Dynamics

In order to consider full transient dynamics for the system, we assume that transmission of infection across a link is a one-step Poisson process, happening at rate τ , and that recovery is Markovian with rate γ . Our methodology is straightforwardly extended to the case where shedding happens at a variable rate during an individual’s infectious period or the case of non-exponentially distributed recovery times through the method of stages (and other compartmental methods). In the Markovian case, $T = \tau/(\tau + \gamma)$, but to calculate $P(i|j)$ we must consider internal dynamics for a subnet of size n with adjacency matrix \mathbf{a} and infection starting on node o . Since the general dynamics in this case are rather hard to write down, we make use of Dirac notation, using the appropriate links to Markov chains [6], to simplify notation.

2.3.1 Within-subnet dynamics

Our starting point is a node-level state space

$$\mathcal{S} = \{|S\rangle, |I\rangle, |R\rangle\} \quad , \quad (11)$$

Defined such that, where we use letters A, B, \dots to represent generic states

$$\langle A|B \rangle = \delta_{A,B} . \quad (12)$$

We then define five abstract operators: three that return the appropriate infection state

$$\begin{aligned} \hat{S}|S\rangle &= |S\rangle, & \hat{S}|I\rangle &= 0, & \hat{S}|R\rangle &= 0, \\ \hat{I}|S\rangle &= 0, & \hat{I}|I\rangle &= |I\rangle, & \hat{I}|R\rangle &= 0, \\ \hat{R}|S\rangle &= 0, & \hat{R}|I\rangle &= 0, & \hat{R}|R\rangle &= |R\rangle; \end{aligned} \quad (13)$$

and two that correspond to transmission and recovery

$$\begin{aligned} \hat{t}|S\rangle &= |I\rangle, & \hat{t}|I\rangle &= 0, & \hat{t}|R\rangle &= 0, \\ \hat{r}|S\rangle &= 0, & \hat{r}|I\rangle &= |R\rangle, & \hat{r}|R\rangle &= 0. \end{aligned} \quad (14)$$

So a general state under consideration obeys

$$|p\rangle \in \mathcal{S}^{\otimes n}, \quad \langle 1|p\rangle = 1, \text{ where } |1\rangle := (|S\rangle + |I\rangle + |R\rangle)^{\otimes n}. \quad (15)$$

This is in contrast to normalisation in quantum mechanics—where states obey $\langle \psi|\psi\rangle = 1$ —and the ‘ket’ $|1\rangle$ is henceforth used without explicit definition to stand for an unweighted sum over basis states. Where $\hat{\mathcal{O}}$ is an operator defined to act on elements of \mathcal{S} , we define an operator acting on the complete state space using subscripting so that

$$\hat{\mathcal{O}}_i := \mathbb{1} \otimes \dots \otimes \underbrace{\hat{\mathcal{O}}}_{i\text{th place}} \otimes \dots \mathbb{1}. \quad (16)$$

Having set up this machinery, we can now write the system’s dynamics in an extremely compact form:

$$\frac{d}{dt}|p\rangle = \hat{Q}|p\rangle, \text{ where } \hat{Q} = \tau \sum_i (\hat{t}_i - \hat{S}_i) \sum_j a_{ij} \hat{I}_j + \gamma \sum_i (\hat{r}_i - \hat{I}_i). \quad (17)$$

Despite this compact expression, the actual dimensionality of the system above grows extremely quickly with network size for numerical and analytical work. There are two general methods available for increasing the tractability of these equations, particularly for final outcomes.

Path integrals for Markov chains

The outcome probabilities for local subnets can be written in terms of the following integral

$$P(j|o) = \int_0^\infty \langle p_j| e^{\hat{Q}t} |o\rangle dt, \quad (18)$$

where we have defined two new states

$$|o\rangle := \hat{I}_o \prod_{j \neq o} \hat{S}_j |1\rangle , \quad |p_j\rangle := \gamma \hat{I}_j |1\rangle . \quad (19)$$

In order to evaluate (18) efficiently, we can make use of the general theory of path integrals for Markov chains [14]. To do this, we need first to decompose the state space into an absorbing set \mathcal{A} and a non-absorbing set \mathcal{C} :

$$\mathcal{S}^{\otimes n} = \mathcal{A} \cup \mathcal{C} , \quad (20)$$

which can be done through the definition of projection operators

$$\begin{aligned} \hat{P}_{\mathcal{A}} &= \sum_{\{A_i\}_{i=1}^n \in \{S,R\}^{\otimes n}} |A_1\rangle \otimes \cdots \otimes |A_n\rangle \langle A_1| \otimes \cdots \otimes \langle A_n| , \\ \hat{P}_{\mathcal{C}} &= \mathbb{1} - \hat{P}_{\mathcal{A}} . \end{aligned} \quad (21)$$

Two further definitions are needed. Firstly, the time evolution operator restricted to the non-absorbing states is given by

$$\hat{Q}_{\mathcal{C}} := \hat{Q} \circ \hat{P}_{\mathcal{C}} . \quad (22)$$

Secondly, in contrast with quantum mechanics, operators are not Hermitian, and so ‘transposed’ operators that act on the adjoint space of ‘bra’ states are denoted using the dagger \dagger and are not identical to the un-daggered operators on ‘ket’ states. Using these definitions, it is possible to write final outcome probabilities for the epidemic process in a particularly compact form:

$$P(j|o) = \langle p_j | ((\hat{Q}_{\mathcal{C}})^{\dagger})^{-1} | o \rangle . \quad (23)$$

This method of path integrals was applied to household epidemic models in [15]. In practice, the inverse operator in (23) need not be calculated in full—for *SIR* dynamics, a matrix representation will exist in which Q is triangular, and so quantities of interest can be calculated by solving a system of triangular linear equations, which is relatively numerically efficient.

Automorphism-driven lumping

Recently, the technique of automorphism-driven lumping has been applied to epidemic dynamics on networks [16] and percolation [8]. This approach reduces the complexity of network problems by making systematic use of discrete symmetries of the network. In particular, the automorphism group of a graph G of size n with adjacency matrix \mathbf{a} is a subset of the permutation group: $\text{Aut}(G) \subseteq S_n$. The elements of the automorphism group leave the adjacency matrix invariant:

$$\mathbf{M} \in \text{Aut}(G) \quad \Leftrightarrow \quad \mathbf{a} = \mathbf{M} \mathbf{a} \mathbf{M}^T . \quad (24)$$

The use of this insight to lump epidemic equations requires some care in the labelling of dynamical variables [16]. Using the notation above, we relabel a generic dynamical state of the system

$$|A_1\rangle \otimes \cdots \otimes |A_n\rangle \equiv |\{(A_1, 1), \dots, (A_n, n)\}\rangle , \quad (25)$$

i.e. we go from an ordered set of states to an unordered set of pairs of states and node numbers. ‘Lumped’ basis states for the dynamical system (17) can then be defined according to the orbits of the automorphism group—this means that states like the above are lumped together into classes like

$$L(A_1, \dots, A_n) = \{ \{(A_1, M(1)), \dots, (A_n, M(n))\} \mid \mathbf{M} \in \text{Aut}(G) \} , \quad (26)$$

where $M(i)$ is the index of the non-zero component of the i -th row of the permutation matrix \mathbf{M} . The dynamical equivalence of these states can be seen by repeated substitution of $\mathbf{a} \rightarrow \mathbf{M}\mathbf{a}\mathbf{M}^T$ into (17). Clearly, lumping classes must contain states that all have the same eigenvalues of \hat{S} and \hat{I} ; and in the limiting case of a fully connected graph such that $\text{Aut}(G) = S_n$, only these aggregate eigenvalues are required to describe the system [16].

2.3.2 Global dynamics

Recently, a set of dynamics was presented that are a manifestly exact description of the mean behaviour of an *SIR* epidemic on a configuration-model network [2] (equivalent to a stubby subnet model where all subnets have one node). We now re-write this in Dirac notation, so that this approach may be readily combined with the within-subnet dynamics above to define exact global dynamics.

Our starting point is a set of states that represent a number of ‘remaining half-links’

$$\mathcal{S} = \{|l\rangle\}_{l=0}^{k_{\max}} , \text{ such that } \langle l' | l \rangle = \delta_{l,l'} , \quad (27)$$

where k_{\max} is the maximum node degree (or more generally maximum number of stubs). We define two operators on such states: a link number operator, and a link-number lowering operator:

$$\hat{l} |l\rangle = l |l\rangle , \quad \hat{l}^- |l\rangle = \begin{cases} |l-1\rangle & \text{if } l \geq 1 , \\ 0 & \text{otherwise.} \end{cases} \quad (28)$$

We now consider how remaining half-links interact with disease state. These are taken as a tensor product,

$$|A, l\rangle = |A\rangle \otimes |l\rangle , \text{ so that } \langle B, l' | A, l \rangle = \delta_{A,B} \delta_{l,l'} . \quad (29)$$

By construction, however, recovered individuals lose all their half-links, so the state space for this system is

$$\mathcal{S} = \{|S, l\rangle, |I, l\rangle, |R, 0\rangle\}_{l=0}^{k_{\max}} . \quad (30)$$

We then define four operators on this space, which we present in terms of their non-trivial action

$$\begin{aligned}
\hat{t}|S, l\rangle &:= (\hat{t}|S\rangle) \otimes |l\rangle = |I, l\rangle , \\
\hat{b}|S, l\rangle &:= (\hat{t}|S\rangle) \otimes (\hat{l}^- |l\rangle) = |I, l-1\rangle , \\
\hat{l}^- |A, l\rangle &:= |A\rangle \otimes (\hat{l}^- |l\rangle) = |A, l-1\rangle , \\
\hat{r}|I, l\rangle &:= |R, 0\rangle .
\end{aligned} \tag{31}$$

Three of these operators are simple uplifts, but the operator \hat{b} for global infection is new. To define the dynamics of this system, we start with a general state

$$|p\rangle = \sum_l (x_l(t) |S, l\rangle + y_l(t) |I, l\rangle) + z(t) |R, 0\rangle , \tag{32}$$

which obeys

$$\langle 1|p\rangle = 1 , \text{ for } |1\rangle := \sum_l (|S, l\rangle + |I, l\rangle) + |R, 0\rangle . \tag{33}$$

There is also a non-linear term for the density of infection amongst free half-links that appears in the system,

$$\rho[p] := \frac{\langle 1|\hat{I}\hat{l}|p\rangle}{\langle 1|\hat{l}|p\rangle} . \tag{34}$$

Then an exact representation of expected *SIR* dynamics on a configuration-model network is given by

$$\begin{aligned}
\hat{Q}[p] &:= \gamma (\hat{r} - \hat{I}) + \tau (\hat{l}^- - \mathbb{1}) \hat{I} + \rho[p] (\gamma + \tau) (\hat{l}^- - \mathbb{1}) \hat{l} + \rho[p] \tau (\hat{b} - \hat{S}) \hat{l} , \\
\frac{d}{dt} |p\rangle &= \hat{Q}[p] |p\rangle .
\end{aligned} \tag{35}$$

The significance of these dynamics is that they do not grow in size with network size; in fact, they are exact in the infinite-size limit, which is inaccessible through simulation or direct integration of (17).

2.3.3 Full system dynamics

For a network made up of stubby subnets, it is possible to make the same construction as above, where global links are made along with the epidemic process. In this case, a general state can be written

$$|p\rangle = \sum_{\sigma, \{A_i, l_i\}_{i=1}^{n_\sigma}} p_{\sigma}^{A_1 \dots A_n}_{l_1 \dots l_n}(t) |\sigma\rangle \otimes |A_1, l_1\rangle \otimes \dots \otimes |A_{n_\sigma}, l_{n_\sigma}\rangle , \tag{36}$$

where $\langle \bar{\sigma}|\sigma\rangle = \delta_{\bar{\sigma}, \sigma}$ as would be expected. Clearly, any attempt to write down differential equations for the tensor representation of this system, $p_{\sigma}^{A_1 \dots A_n}_{l_1 \dots l_n}(t)$,

will involve extremely complex expressions. By contrast, using the formalism of Dirac notation and operators that we have developed above, we can write the exact dynamics for this system as

$$\begin{aligned}
\hat{P}_\sigma &:= \sum_{\{A_i, l_i\}_{i=1}^{n_\sigma}} |\sigma\rangle \otimes |A_1, l_1\rangle \otimes \cdots \otimes |A_{n_\sigma}, l_{n_\sigma}\rangle \langle A_{n_\sigma}, l_{n_\sigma}| \otimes \cdots \otimes \langle A_1, l_1| \otimes \langle \sigma| \\
\rho[p] &:= \frac{\langle 1 | \sum_\sigma \sum_{i=1}^{n_\sigma} \hat{I}_i \hat{l}_i \hat{P}_\sigma | p \rangle}{\langle 1 | \sum_\sigma \sum_{i=1}^{n_\sigma} \hat{l}_i \hat{P}_\sigma | p \rangle} , \\
\hat{Q}[p] &:= \gamma \sum_i \left(\hat{r}_i - \hat{I}_i \right) + \tau \sum_i \left(\hat{l}_i^- - \mathbb{1} \right) \hat{l}_i \hat{I}_i + \tau \sum_i \left(\hat{t}_i - \hat{S}_i \right) \sum_{\sigma, j} a_{ij}^\sigma \hat{I}_j \hat{P}_\sigma \\
&\quad + \rho[p] (\gamma + \tau) \sum_i \left(\hat{l}_i^- - \mathbb{1} \right) \hat{l}_i + \rho[p] \tau \sum_i \left(\hat{b}_i - \hat{S}_i \right) \hat{l}_i , \\
\frac{d}{dt} |p\rangle &= \hat{Q}[p] |p\rangle .
\end{aligned} \tag{37}$$

These equations have the same significance as above: the exact expected epidemic dynamics of a class of clustered dynamics can be calculated for the infinite-size limit of a network.

3 Examples

We now turn to some examples of the methodology presented above to specific networks. Throughout this section we work in natural units such that the recovery rate $\gamma = 1$.

3.1 Invasion and final size

We consider invasion on the two locales shown in Figure 1. These networks are constructed from the envelope / diamond motif as shown, so that every individual has exactly n links. This means that all differences between this model and an n -regular random graph derive from the presence and structure of short loops in the network and not heterogeneity in node degree. The locale basic reproductive ratio is given by:

$$\begin{aligned}
R_L &= \left(\tau(2(n-3)^2 + (n(25n-142) + 204)\tau + (n(133n-716) + 982)\tau^2 \right. \\
&\quad \left. + (n(377n-1948) + 2570)\tau^3 + (n(563n-2846) + 3672)\tau^4 \right. \\
&\quad \left. + 2(n(193n-968) + 1239)\tau^5 + 12(8(n-5)n + 51)\tau^6) \right) \\
&\quad / ((2n-5)(1+\tau)^4(1+2\tau)^2(1+3\tau)) . \tag{38}
\end{aligned}$$

Final sizes are calculated using (10). In Panes (c) and (d) of Figure 1, to compare the asymptotically exact results (blue line) with finite-size networks, 10^6 Simulations were run for envelope-based networks of size 100 and 1000, with $n = 4$, over a range of transmission parameter values. For comparison,

theoretical curves were also plotted for a configuration model where every node has four links (red line), and a household model for households of size 4 where every individual has one stub (green line). Final sizes for these two comparators are a special case of the analysis in [3, 4]. Clearly, all of these comparator networks also have the property that neighbourhood sizes are uniformly equal to four, and so all outcome differences are due to local clustering structure.

The results shown in Panes (c) and (d) of Figure 1 show firstly that this local clustering structure does have a significant impact on epidemic outcomes, and also that even for relatively small networks the results of simulation demonstrate this difference and agree well with the asymptotic result. The blue line representing final outcomes also has two interesting features: there is a short plateau of small but finite final sizes above the invasion threshold; and for very fast transmission, the predicted final sizes are larger than for the unclustered regular graph.

3.2 Full Dynamics

While invasion thresholds are of practical interest, transient dynamical features of epidemics are also important, and are not always simply determined by consideration of thresholds. Figure 2 shows the exact transient behaviour for two special graphs, both of which give all nodes degree three: (a) a configuration-model network where each node has 3 stubs; (b) a stubby-subnet graph composed of triangles with each node having one stub. The dynamics as defined above give the epidemic curves shown in (c) for the CM network and (d) for the triangle-based network respectively.

These show the interesting feature that once we are in a region of much faster transmission than is required for invasion, the clustered network exhibits later but higher peaks—an analogue of the larger final sizes seen for clustered networks at very large τ above.

4 Other solvable networks

It has been clear for some time that a network (or otherwise structured population) with a local-global distinction will admit a solution to an epidemic on that network [1]. As a practical adjunct to this, both the local and global features of the network must individually admit solution. The stubby-subnet networks here propose one such distinction: each node can be uniquely assigned to a local unit of clustered structure; and global mixing happens through a configuration model network.

We now consider three other versions of this concept, firstly by introducing assortative mixing outside the subnet, secondly using the recently defined role-based networks, and finally to weighted networks.

4.1 Assortativity

In [12], a generalisation of the configuration model was developed to incorporate the notion of assortativity. Such assortativity (or even disassortativity) is a mainstay of epidemiology, and much theoretical effort has been expended to model its effects [5]. To describe assortativity, we introduce a correlation matrix $C_{\bar{\lambda},\lambda}$ (analogous to the e_{kl} of [12]) that multiplies the probabilities that two locales are linked globally compared to the configuration model. For such a network, the locale next generation matrix is

$$\mathcal{K}_{\lambda\lambda}^L = T \frac{M_{\bar{\sigma}} s_{\bar{o}}^{\bar{\sigma}}}{s_{\text{tot}}} \left((s_o - 1) C_{\bar{\lambda},\lambda} + \sum_{j \in v_{\sigma} \ominus o} P_{\sigma}(j|o) s_j C_{\bar{\lambda},(\sigma,j)} \right), \quad (39)$$

and an appropriate threshold parameter will be given by the dominant eigenvalue of this matrix. Exact transient dynamics for such a system should also be straightforward to write down: in addition to indexing a node with its effective remaining half-links and disease state, each node should also be indexed by locale. Instead of having homogeneous transmission on the basis of pairing half-links at rate τ , the rate should then be multiplied by $C_{\bar{\lambda},\lambda}$. Of course, this yields equations that are at least quadratic rather than linear in maximum node degree, making numerical integration correspondingly more difficult.

4.2 Role-based networks

Role-based networks as considered in [13, 10, 8] involve a different definition of local and global. In these networks, it is links that can be uniquely assigned to a local unit of clustered structure, meaning that nodes can be attached to many different clustered subgraphs. This clearly allows a next-generation matrix to be established by indexing cases by the unit of structure through which they acquired infection, as in [10]. The definition of manifestly exact dynamics is less clear in this case, however dynamical approaches such as [18] that are in extremely good numerical agreement with simulation, and may turn out to be exact through further work, can clearly be extended to role-based networks. The primary differences between stubby-subnet and role-based networks are that the former can specify an exact structure of stubs for each node in a clustered motif, while the latter can involve each node in several motifs. As such, these are best seen as complementary approaches to the fast-moving field of solvable clustered networks.

4.3 Weighted networks

While all networks discussed above have been topological (i.e. links are either present or not) all of the analysis above carries through exactly if within-subnet links are weighted, so $a_{ij}^{\sigma} \in \mathbb{R}$. It is also possible to stratify global links into multiple contexts, each with a given strength (i.e. different values of T) although

this latter modification does increase the system dimensionality, while weighting within-subnet dynamics does this only if the weighting breaks a discrete symmetry of the topological network.

Acknowledgements

Work funded by the UK Engineering and Physical Sciences Research Council (Grant Number EP/H016139/1). The author would like to thank Matt Keeling and Josh Ross for helpful discussions and comments on this work.

References

- [1] F. BALL AND P. NEAL, *A general model for stochastic SIR epidemics with two levels of mixing*, Mathematical Biosciences, 180 (2002), pp. 73–102.
- [2] ———, *Network epidemic models with two levels of mixing*, Mathematical Biosciences, 212 (2008), pp. 69–87.
- [3] F. BALL, D. SIRL, AND P. TRAPMAN, *Threshold behaviour and final outcome of an epidemic on a random network with household structure*, Advances in Applied Probability, 41 (2009), pp. 765–796.
- [4] ———, *Analysis of a stochastic SIR epidemic on a random network incorporating household structure*, Mathematical Biosciences, 224 (2010), pp. 53–73.
- [5] O. DIECKMANN AND J. HEESTERBEEK, *Mathematical Epidemiology of Infectious Diseases: Model Building, Analysis and Interpretation*, J Wiley, 2000.
- [6] P. J. DODD AND N. M. FERGUSON, *A many-body field theory approach to stochastic models in population biology*, PLoS ONE, 4 (2009), p. e6855.
- [7] T. HOUSE, G. DAVIES, L. DANON, AND M. J. KEELING, *A motif-based approach to network epidemics*, Bulletin of Mathematical Biology, 71 (2009), pp. 1693–1706.
- [8] B. KARRER AND M. E. J. NEWMAN, *Random graphs containing arbitrary distributions of subgraphs*, arXiv:1005.1659v1, (2010).
- [9] M. J. KEELING, *The effects of local spatial structure on epidemiological invasions*, Proc Biol Sci, 266 (1999), pp. 859–67.
- [10] J. MILLER, *Percolation and epidemics in random clustered networks*, Physical Review E, 80 (2009), pp. 1–4.
- [11] M. MOLLOY AND B. REED, *A critical point for random graphs with a given degree sequence*, Random Struct. Algorithms, 6 (1995), pp. 161–179.

- [12] M. NEWMAN, *Assortative mixing in networks*, Physical Review Letters, 89 (2002), p. 208701.
- [13] M. NEWMAN, *Random graphs with clustering*, Physical Review Letters, 103 (2009), pp. 1–4.
- [14] P. K. POLLETT AND V. E. STEFANOV, *Path integrals for continuous-time Markov chains*, J. Appl. Prob., 39 (2002), pp. 901–904.
- [15] J. V. ROSS, T. HOUSE, AND M. J. KEELING, *Calculation of disease dynamics in a population of households*, PLoS ONE, 5 (2010), p. e9666.
- [16] P. L. SIMON, M. TAYLOR, AND I. Z. KISS, *Exact epidemic models on graphs using graph automorphism driven lumping*. Sussex Maths Preprint: SMRR-2010-02. Published online at the Journal of Mathematical Biology ahead of print, 2010.
- [17] P. TRAPMAN, *On analytical approaches to epidemics on networks*, Theoretical Population Biology, 71 (2007), pp. 160–173.
- [18] E. M. VOLZ, *Dynamics of infectious disease in clustered networks with arbitrary degree distributions*, arXiv:1006.0970v1, (2010).

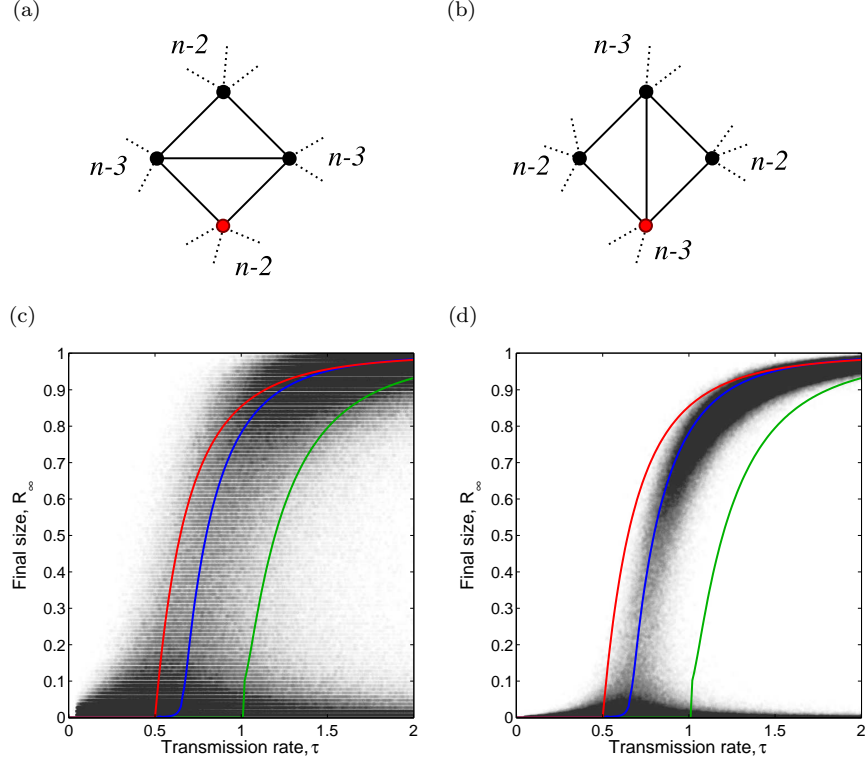


Figure 1: Epidemics on envelope / diamond motif-based networks. (a) and (b) show the two locales involved. Bottom panes show final sizes for 10^6 simulations on networks of size (c) 100 and (d) 1000. Each translucent dot represents a realisation; blue lines are asymptotic predictions for a regular graph of degree 4; red lines are the asymptotic predictions for the envelope network with $n = 4$; and green lines are asymptotic predictions for four-cliques with one global link per node.

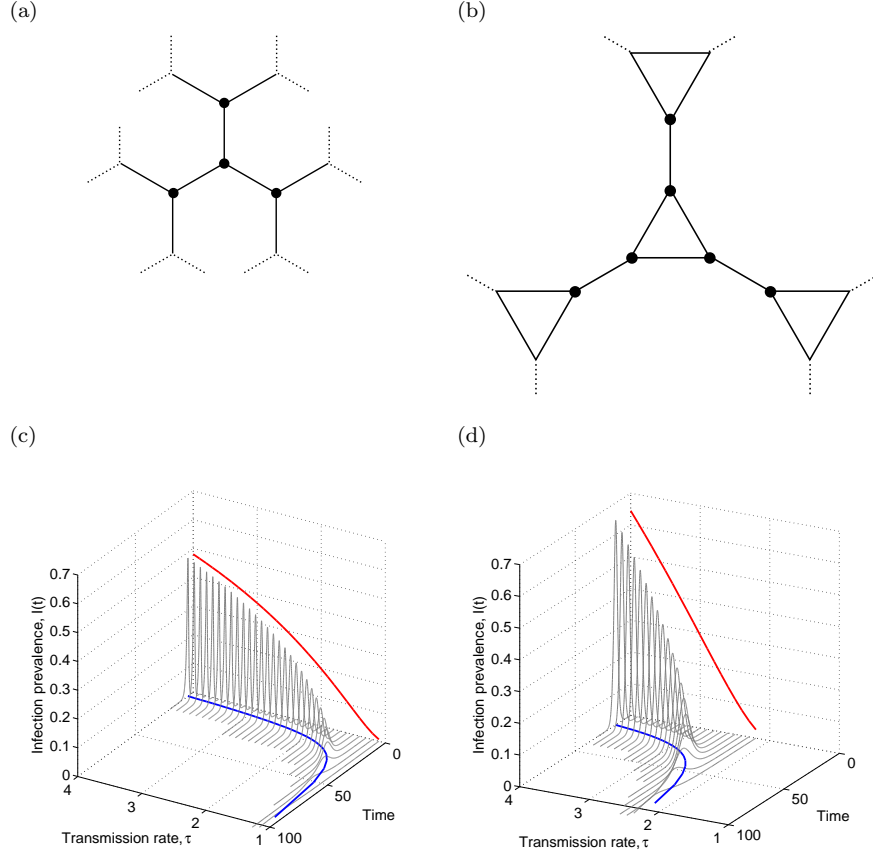


Figure 2: Exact transient epidemic dynamics for two special networks. (a) shows a typical location in the unclustered graph, and (b) shows a typical location in the clustered graph. Epidemic curves (grey) for different parameter values are shown in (c), (d) respectively. Peak times (blue) and peak heights (red) are projected onto the appropriate axes.